Identification of antimalarial targets of chloroquine by a combined deconvolution strategy of ABPP and MS-CETSA

Peng Gao
China Academy of Chinese Medical Sciences Institute of Chinese Materia Medica
Yanqing Liu
China Academy of Chinese Medical Sciences Institute of Chinese Materia Medica
Wei Xiao
Southern Medical University
Fei Xia
China Academy of Chinese Medical Sciences Institute of Chinese Materia Medica
Jiayun Chen
China Academy of Chinese Medical Sciences Institute of Chinese Materia Medica
Liwei Gu
China Academy of Chinese Medical Sciences Institute of Chinese Materia Medica
Fan Yang
Shenzhen People's Hospital
Liuhai Zheng
Shenzhen People's Hospital
Junzhe Zhang
China Academy of Chinese Medical Sciences Institute of Chinese Materia Medica
Qian Zhang
China Academy of Chinese Medical Sciences Institute of Chinese Materia Medica
Zhijie Li
Shenzhen People's Hospital
Yuqing Meng
China Academy of Chinese Medical Sciences Institute of Chinese Materia Medica
Yongping Zhu
China Academy of Chinese Medical Sciences Institute of Chinese Materia Medica
Chengchao Xu
China Academy of Chinese Medical Sciences Institute of Chinese Materia Medica
Lingyun Dai
Shenzhen People's Hospital
Jigang Wang (jgwang@icmm.ac.cn)

Southern Medical University https://orcid.org/0000-0002-0575-0105

Research

Keywords: chloroquine, antimalaria, ABPP, CETSA, quantitative proteomics

Posted Date: November 19th, 2021

DOI: https://doi.org/10.21203/rs.3.rs-958967/v1

Abstract

Background

Malaria is a devastating infectious disease that disproportionally threatens hundreds of millions of people in developing countries. In the history of anti-malaria campaign, chloroquine (CQ) has played an indispensable role, however, its mechanism of action (MoA) is not fully understood.

Methods

We used the approach of photo-affinity labeling (PAL) in the design of a chloroquine probe and developed a combined deconvolution strategy – activity-based protein profiling (ABPP) and mass spectrometry-coupled cellular thermal shift assay (MS-CESTA) – that identified the protein targets of chloroquine in an unbiased manner in this study.

Results

We developed a novel photo-affinity chloroquine analog probe (CQP), which retains the antimalarial activity in the nanomole range, and identified a total of 40 proteins that specifically interacted and photo-crosslinked with CQP, which was inhibited in the presence of excess CQ. Using MS-CETSA, we identified 83 candidate interacting proteins out of a total of 3375 measured parasite proteins. Together, we identified 8 proteins as the most potential hits which were commonly identified by both methods.

Conclusions

We found that CQ could disrupt glycolysis and energy metabolism of malarial parasites through direct binding with some of the key enzymes, a new mechanism that is different from its known inhibitory effect of hemozoin formation. This is the first report of identifying chloroquine antimalarial targets by a parallel usage of labeled (ABPP) and label-free (MS-CETSA) methods.

Background

Malaria is an ancient lethal infectious disease that is still widely distributed in nearly 90 countries – mostly developing countries – around the world [1, 2]. According to the World Malaria report, there were about 229 million malaria infection cases in 2019, claiming 409000 lives [3]. In the history of antimalarial drug development, the discovery of chloroquine (CQ) represented a major breakthrough and chloroquine has played an essential role in the past anti-malaria campaign [4]. As a long-acting, cost-effective, and well-tolerated drug, chloroquine is still prescribed to prevent and treat the infection of *Plasmodium vivax*, *P. ovale*, *P. malariae*, and *P. knowlesi*, but not *P. falciparum* – in which chloroquine resistance

unfortunately becomes a widespread phenomenon [5]. Moreover, CQ is also used to treat autoimmune disorders like rheumatoid arthritis and lupus erythematosus [6].

CQ is a diprotic weak-basic drug (pKa1 = 8.1, pKa2 = 10.2) that exist in both protonated and unprotonated forms [7, 8]. Once entering the digestive vacuole (DV) of the parasite, CQ becomes protonated and charged, resulting in its trapping and accumulation inside this acidic organelle [8]. The nutrients required for the propagation of parasites comes from vacuolar digestion of haemoglobin, generating high levels of the toxic byproduct heme [9]. Malarial parasites rely on the formation of hemozoin to crystalize and sequester heme [10]. Interestingly, this detoxification process is disrupted by CQ binding, which destroys membrane function and integrity, and ultimately leads to cell death [6]. Besides, recombinantly expressed *P. falciparum* lactate dehydrogenase (*Pf*LDH) and tyrosinase were reported to bind to CQ, suggesting CQ might also target other proteins in malaria [11, 12]. However, there is no study that systematically profiles the protein targets of CQ in malarial parasites at the proteome level.

Here, we used the activity-based protein profiling (ABPP) technology [13–15] in combination with mass spectrometry-coupled cellular thermal shift assay (MS-CETSA) [16–20] to systematically identify the target proteins of CQ underlying its antimalarial effect.

Methods

Synthesis of CQP

Synthetic steps and intermediate products of CQP as seen in Supplementary materials.

Parasite culture

The *Plasmodium falciparum* 3D7 strain was obtained from Artemisinin Research Center of China, Academy of Chinese Medical Sciences. *P. falciparum* 3D7 was cultured in malaria culture media (MCM) containing 10.4 g/L RPMI 1640, 0.5% albumin, 0.2 g/L gentamycin, 25 μg/mL hypoxanthine, 0.3 g/L L-glutamine, 25 mM HEPES, 2.5 g/L $NaHCO_3$ and supplement of 2% healthy human erythrocytes provided by Beijing Red Cross Blood Center. The parasites were maintained at 37°C with 5% CO_2, 5% O_2, and 90% N_2. Giemsa-stained thin blood smears were performed to evaluate the parasite growth status and parasitemia.

Drug antimalarial activity assay

The antimalarial activities of CQP were measured using a standard 72 h fluorescent SYBR Green I based assay as described previously with slight modifications to determine the half-maximal inhibitory concentration (IC_{50}) against *P. falciparum* 3D7 strain. Briefly, parasites were synchronized using 5% sorbitol twice, and then the highly synchronized ring-stage parasites were prepared at 2% hematocrit and 0.5% parasitemia. The parasite cultures were incubated with 3-fold serially diluted concentrations of compounds starting from 30 μM in 96-well microplates for 72 h at 37°C with 5% CO_2, 5% O_2, and 90% N_2. Subsequently, 100 μL lysis buffer (30 mM Tris pH 7.5, 10 mM EDTA, 0.01% saponin, 0.08% Triton X-100)

containing 2 × SYBR Green I was added in each well for 1.5 h in dark at 37 ℃. Then, the fluorescence was measured using EnVision 2105 Multimode Plate Reader (PerkinElmer) with λex = 485 nm, λem = 535 nm. Uninfected erythrocytes and drug-free infected erythrocytes (0.5% parasitemia) with the same hematocrit served as blank control and negative control, respectively. At least three biological replicates and technical replicates were performed for each drug doses. The IC_{50} was calculated and dose–response curve fitting of the % inhibition VS log[dose] was performed using the GraphPad Prism 8 software.

In situ **fluorescence labeling assay of** P. falciparum

P. falciparum parasites (unsynchronized) were cultured to ~ 10% parasitemia with 2% hematocrit. The parasites were incubated with 10 volumes of cold 0.05% saponin containing 1 × Protease inhibitor (PI, Thermo Scientific) for 10 min on ice in order to be released from erythrocytes. Then the lysates were centrifuged at 4000 rpm for 1 min at 4 ℃ followed by discarding the supernatant. The parasite pellets were washed 3 times with 10 volumes of pre-chilled PBS containing 1 × PI in order to completely remove host erythrocyte proteins. The pellet was resuspended with lysis buffer containing 1 × PI, 50 mM HEPES, 5 mM β-glycerophosphate, 0.1 mM activated Na_3VO_4, 20 mM $MgCl_2$, 1 mM TCEP. The parasite pellets were subjected to 3 cycles of flash-freeze–thawing in liquid nitrogen and room temperature water, followed by brief sonication on ice water. Then the lysates were centrifuged at 12,000 rpm for 10 min at 4 ℃. The soluble protein fraction in the supernatant was collected and the protein concentrations were determined using Bicinchoninic Acid Protein Assay Kit (BCA, Thermo Scientific). A serial of the equal amount of soluble protein lysates (50 μg) was incubated with increasing concentrations (10 ~ 2000 nM) of CQP dissolved in DMSO for 4 hours at room temperature, and equal volume DMSO was served as blank control with a final concentration of 0.1%. For competition assay, the protein lysate was pre-treated with 100-fold of chloroquine for 1 h, followed by incubation with CQP (2 μM) for 4 h. Then, the samples were irradiated with UV light (λ = 365 nm) for 10 min on ice, and the unirradiated samples with the same treatment were used as parallel negative control. Then, the samples were labeled with fluorescent tag through click chemistry reaction (CuAAC). TBTA (100 μM in DMSO), TCEP (1 mM in water), $CuSO_4$ (1 mM in water) and TAMRA-azide (50 μM in DMSO) were sequentially added to the lysates and incubated at room temperature (RT) for 2h with rotating. Pre-chilled ice acetone was added to precipitate the proteins, and volatilized after high-speed centrifugation. Then, 30 μL 1 × SDS-PAGE Loading buffer was added to dissolve the proteins by sonication and heating for 10 min at 95°C. 10 μL per sample was loaded onto 10% acrylamide gel to separate proteins by electrophoresis. The fluorescence scanning and analysis were performed using Sapphire Biomolecular Imager (Azure Biosystems).

Pull down experiment and targets identification

The extraction of parasite proteins was carried out same as described above. The parasite lysate (500 μg) was incubated with CQP (2 μM) for 4 h at RT, and the lysate with equal volume of DMSO was used as a negative control. A competition assay was performed by pretreating the lysate with 200 μM chloroquine for 1 h before incubating with CQP for another 4 h. Then, the samples were irradiated with UV light (λ =

365 nm) for 10 min on ice. The reactions were stopped by adding eight volumes of pre-chilled acetone followed by centrifugation at 4000 rpm for 10 min. The unreacted chloroquine and CQP probe were removed during the protein precipitation step. The pellets were then dissolved in 0.16% SDS in PBS buffer and click chemistry was carried out to conjugate the biotin tag with proteins. For each sample, TBTA (100 μM in DMSO), TCEP (1 mM in water), CuSO4 (1 mM in water) and biotin-azide (50 μM) were sequentially added to the lysates and incubated at RT for 2 h with rotating. Then samples were precipitated with acetone again and redissolved in 0.1% SDS in PBS, followed by incubation with 60 μl NeutrAvidin beads (Thermo Scientific) at RT for 4 h with gentle rotation. The beads were then washed with 1% SDS, 6 M urea and 1 × PBS three times, respectively, and incubated with denaturation and reduction buffer containing 500 μl 6 M urea and 25 μl of 100 mM DTT for 30 min at 37 ℃, followed by alkylation with 25 μl of 400 mM iodoacetamide (IAA) in dark for 30 min at RT. For digestion, beads were resuspended in 150 μl 2 M urea with 1 mM $CaCl_2$ and 3 μg trypsin (0.5 μg/μl), which were then incubated at 37 ℃ overnight with shaking. After the digestion, the samples were centrifuged and supernatants were collected. The supernatants containing peptides were desalted using C18 column (Waters, USA) and the peptides were eluted with 1% formic acid in 70% acetonitrile, and then dried in a centrifugal vacuum evaporator. Samples were redissolved in 100 mM TEAB and labeled with TMT10plex Labeling Reagents (Thermo Scientific) for 4 h at RT, followed by desalting with C18 column again. Samples were resuspended in buffer containing 1% formic acid and 1% acetonitrile, and peptides were analyzed by LC-MS/MS.

LC-MS/MS analysis

LC-MS/MS analyses were performed on an UltiMate 3000 RSLC nano LC system coupled with an Orbitrap Fusion Lumos Mass Spectrometer (Thermo Fisher Scientific). Dried peptide sample fractions were reconstituted in 10 μL 0.1% formic acid and 1% acetonitrile, transferred to 96-well plate autosampler. 2 μL of each reconstituted fraction was loaded into an Acclaim™PepMap™100 C18 Nano-Trap Columns (100 Å, 3 μm, 75 mm × 2 cm) and washed with 0.5% formic acid and 2% acetonitrile at a flow rate of 5 μL/min for 5 min. The peptides were separated on an Acclaim™ PepMap™100 C18 HPLC reversed-phase analytical column (130 Å, 2 μm, 75 μm × 250 mm) using a 75 min gradient elution with solvent A of 0.1% formic acid aqueous solution and solvent B of 0.1% formic acid in 80% acetonitrile starting from 2% up to 90% mobile phase solvent B with a flow of 0.3 μL/min at 40°C. The mass spectrometer was operated using Xcalibur software (version 4.2.4 SP1) in the data-dependent acquisition mode with NSI (nano spray ion source) spray voltage of 2.5 kV, capillary temperature of 300°C and RF Lens of 30%. All MS spectra detection was performed in positive-ion mode with charge states of 2 ~ 6 included, using orbitrap detector with a full scan MS spectra from m/z 300 ~ 1500 in the FTMS (Fourier Transform Mass Spectrometry) mode at 60,000 resolution. For each MS spectrum, multiply charged ions over the selected intensity threshold 2.5e4 were selected for MS/MS in cycles of 3 seconds. The top 20 most abundant precursors were subjected to HCD with collision energy of 38% in the ion trap with a fixed first mass of 110 m/z at 50,000 resolution and with isolation window of 0.7 m/z.

The original mass spectrometry data collected by Xcalibur analysis system were searched and analyzed by Proteome Discoverer version 2.4 (Thermo Fisher Scientific), and the peptide matching and protein

identification were carried out by Sequest HT algorithm against *P.falciparum* 3D7 protein database (PlasmoDB-50, https://plasmodb.org/plasmo/app/downloads/release-50/P.falciparum3D7/fasta/data/), uniprot human protein database (reviewed_20200112), common contaminated protein database (ftp://ftp.thegpm.org/fasta/cRAP). The PD search parameters were set as follows: The precursor mass tolerance was set to 15 ppm and fragment mass tolerance to 0.02 Da. Carbamidomethyl/+57.021Da (C) and Oxidation/+15.995 Da (M) were set as static modification, Deamidated/+0.984 Da (N, Q) was set as dynamic modification and Acetyl/+42.011 Da was set as protein N-terminal dynamic modification. Trypsin(full) was set as proteolytic enzyme with a maximum of two missed cleavages sites allowed. The minimum peptide length was set to 6. Peptide spectra matches were filtered with FDRs of 1% (Strict) and 5% (Relaxed) on the peptide-spectrum match and subsequently on the protein level.

Sample preparation for MS-CETSA-ITDR and targets identification

The MS-CETSA-ITDR assay was performed to identify the targets protein as described previously with slight modification. The parasite lysate used in this assay was similarly prepared as described above. After the protein quantification using BCA kit, lysate aliquots of equal volume were incubated with increasing concentrations of CQ (0, 0.01, 0.1, 1, 5, 25, 100, 300 μM) for 3 min at room temperature, followed by dividing each sample into 3 equal portions into PCR tubes, respectively. The samples were heated at 37 ℃, 52 ℃ or 61 ℃ for 3 min, followed by cooling at 4 ℃ for 3 min. The heated samples were centrifuged at 21,000 g for 30 min at 4°C, and the supernatant was collected. The protein concentrations were determined using BCA assay. For each set of samples under one heating temperature, a certain volume of 30 μg protein per sample was transferred into new 1.5 mL tubes. The denaturation and reduction treatment was initiated by adding 20 mM TCEP, 0.05% RapiGest and 100 mM TEAB to each sample, heating for 20 min at 55 ℃ with continuous shaking. The alkylation step was carried out with 55 mM CAA and incubated for 30 min at RT in dark. Each sample was supplemented with 100 mM TEAB to reduce the RapiGest concentration to 0.025%, after which 1 μg LysC was added and incubated with samples for 3 h at 37 ℃ with shaking at 200rpm. Samples were then digested with 3 μL trypsin (0.5 μg/μL) at 37°C for 18 hours on a rotatory shaker at 200 rpm. After digestion, TFA was added to the digested samples to the final concentration of 1% in order to hydrolyze RapiGest by incubation at 37°C for 45 minutes. Samples were centrifuged at 21,000 g for 15 min at RT and the supernatants containing peptides were transferred into new 1.5 mL tubes, dried with a centrifugal vacuum evaporator at 60°C. Peptides were redissolved in 200 μL 100 mM TEAB and dried again. The redissolution and spinning-vacuum-drying were repeated until pH was maintained at 8.5.

For the TMT-labeling, each peptide sample of 10 μg was labeled with TMT10plex reagents for 2 h in dark at room temperature. The labeling reactions were quenched by adding 25 μL of 1 M Tris-HCl (pH 8.0). Then the labeled samples were combined and desalted using Oasis HLB column as described previously. Briefly, Oasis HLB column was equilibrated with 1 mL 100% acetonitrile, washed with 1 mL of 0.1% formic acid for 3 times. Then, the pooled peptide sample was loaded onto the column and washed with 1 mL of 0.1% formic acid for 5 times. The peptide was eluted with 1 mL of 0.1% acetic acid, 60%

acetonitrile, followed by drying with a centrifugal vacuum evaporator at 60°C. The sample was resuspended in 40 µL of 5% acetonitrile and 5% ammonia buffer, vortexed and centrifuged at 21,000 g for 30 min at room temperature. Then peptide offline prefractionation was carried out using Nexera LC-40D XS liquid chromatography system equipped with a high-pH reversed-phase XBridge Peptide BEH C18 Column (130 Å, 3.5 µm, 4.6 mm X 250 mm). Gradient elution was carried out with buffer A 10 mM ammonium formate (pH 10.0) and buffer B 10 mM ammonium formate (pH 10.0) in 80% acetonitrile. 35 µL of sample was injected into the system and separated on the high-pH reversed-phase column using a 120 min gradient elution (10 min to 5% B, 60 min to 40% B, 40 min to 80% B and 10 min in 80% B) at a constant flow rate of 0.5 mL/min at 40 ℃. The fractions of 15 min ~ 110 min were collected in a 96-well deep-well storage plate. Finally, the samples were pooled to generate 20 fractions. Peptide fractions were dried in a centrifugal vacuum evaporator at 60°C, followed by washing with 100 µL of 0.1% formic acid in 60% acetonitrile twice to remove residual ammonium formate. The samples were then subjected to follow-up LC-MS/MS analysis. And the original mass spectrometry data was analysed as above LC-MS/MS analysis mentioned.

The mineCETSA package (https://github.com/nkdailingyun/mineCETSA) was used to analyze and visualize the CETSA data from PD search. The data were read-in, cleaned, normalized, curve fitted and visualized in RStudio. We applied an array of stringent criteria for high – confident hits selection of CETSA-ITDR, including: ΔAUC ≥ 3 × MAD (AUC : area under the curve; MAD : median absolute deviation) of heat-challenged sample normalized against nondenaturing 37°C control, the maximal fold change (FC ≥1.3) of relative protein abundance in at least one drug dose–treated sample relative to the control sample protein level, the dose-response curve best-fitting quality ($R^2 \geq 0.85$), the Slope of dose-response curve > 0.25 and MDT (mininal dose threshold) < 5 µM.

Target validation using western blotting

Western blotting was performed to validate the pull-down targets. The samples (CQP, DMSO and competition sample) were washed with 1% SDS, 6 M urea and 1 × PBS three times, respectively and the enriched proteins were eluted from beads with 1 × SDS-loading buffer, followed by boiling at 96 ℃ for 10 min. The samples then were centrifugated and the supernatants were separated via SDS-PAGE gel, and the proteins were wet transferred onto PVDF membranes. The membranes were blocked with 5% skim milk solution, followed by incubation with primary and secondary antibody, respectively, as indicated. Subsequently the samples were visualized using High-sig ECL Substrate (Tanon, China).

Recombinant protein expression and purification

The gene of L-lactate dehydrogenase (*Pf*LDH, *PF3D7_1324900*), ornithine aminotransferase (*Pf*OAT, *PF3D7_0608800*), pyruvate kinase (*Pf*PyrK, *PF3D7_0626800*), phosphoglycerate kinase (*Pf*PGK, *PF3D7_0922500*) and triosephosphate isomerase (*Pf*TPI, *PF3D7_1439900*) of *P. falciparum* 3D7 were synthesized commercially with codon-optimization and were cloned into vector pET-28a. The plasmids were transformed into *E. coli* strain BL21. The cells were cultured in LB medium till OD600 reached ~ 0.8, and the protein expression was induced with 0.5 mM isopropyl b-D-thiogalactoside at 16°C for 16 h. Cells

were collected by centrifugation and resuspended in buffer A (50 mM HEPES pH 7.5, 300 mM NaCl, 5 mM b-mercaptoethanol, 1 mM PMSF) and disrupted at 12,000 p.s.i. using a JN-Mini Pro homogenizer (JNBio, China). Whole cells and cell debris were removed by centrifugation at 16,000 rpm and the supernatant was loaded onto a Ni-NTA affinity column (Thermo Scientific). The columns were washed with buffer A containing 30 mM imidazole, and the recombinant protein samples were eluted with buffer B (50 mM HEPES pH 7.5, 150 mM NaCl, 150 mM imidazole). The imidazole was removed using Zeba^{TM} Spin Desalting Columns (Thermo Scientific).

In vitro **fluorescence labeling of** P. falciparum **3D7 recombinant proteins**

The recombinant proteins (2 μg) were incubated with CQP (2 μM) for 4 h at RT, and the protein samples with equal volume of DMSO added was used as negative control. A competition assay was performed by pretreating the proteins with 200 μM chloroquine for 1 h before incubating with CQP (2 μM) for another 4 h. After the incubation, click chemistry was carried out and for each sample, TBTA (100 μM in DMSO), TCEP (1 mM in water), CuSO4 (1 mM in water) and TAMRA-azide (50 μM) was sequentially added in the samples and incubated at RT for 2h with rotating. Then samples were precipitated with acetone and the pellets were redissolved in 0.1% SDS in PBS, followed by the incubation with fluorescent dye. Samples were separated via SDS-PAGE gel and visualized by a laser scanner (Azure Biosystems, USA).

LDH activity assay

The LDH Assay Kit (Beyotime, China) was used to monitor the activity of *Pf*LDH protein. Purified *Pf*LDH (0.5 μg) was first incubated with different concentrations of chloroquine (0 ~ 25 μM) at 28 ℃ for 1 h. Afterwards, the mixture was transferred into a 96-well plate, and the LDH detection buffer was then added, followed by continuous detection of absorbance at 490 nm with a multimode plate reader (PerkinElmer, USA). The reaction buffer with chloroquine but no LDH served as negative control. The measurements were carried out in triplicate.

OAT activity assay

The δ-OAT Activity Detection Assay Kit (Solarbio, China) was applied to monitor the activity of *Pf*OAT protein. Purified *Pf*OAT protein (0.2 μg) was first incubated with different concentrations of chloroquine (0 ~ 100 μM) at 28 ℃ for 1 h. The resulting mixture was then transformed into a 96-well plate, and the substrate NADH and OAT reaction buffer were then added, followed by continuous detection of NADH absorbance at 340 nm with a multimode plate reader (PerkinElmer, USA). The reaction buffer with chloroquine but no OAT served as negative control. The measurements were carried out in triplicate.

Pyruvate kinase activity assay

The Pyruvate Kinase (PK) Assay Kit (Abcam, England) was used to monitor the activity of *P. falciparum* pyruvate kinase (*Pf*PyrK). Purified *Pf*PyrK protein (0.5 μg) was first incubated with different concentrations of chloroquine (0 ~ 40 μM) at 28 ℃ for 1 h. The resulting mixture was then transformed into a 96-well plate, the assay buffer and substrate mix were added in followed by continuous detection of absorbance at 570 nm with a multimode plate reader (PerkinElmer, USA). The reaction buffer with

chloroquine but no pyruvate kinase served as negative control. The measurements were carried out in triplicate.

PGK activity assay

The Phosphoglycerate Kinase Activity Assay Kit (Abcam, England) was applied to monitor the activity of *Pf*PGK protein. Purified *Pf*PGK protein (0.5 μg) was first incubated with different concentrations of chloroquine (0 ~ 100 μM) at 28 ℃ for 1 h. The resulting mixture was then transformed into a 96-well plate, and the reaction mix buffer (including PGK substrate and developer, ATP and NADH) was then added, followed by continuous detection of NADH absorbance at 340 nm with a multimode plate reader (PerkinElmer, USA). The reaction buffer with chloroquine but no *Pf*PGK served as negative control. The measurements were carried out in triplicate.

TPI activity assay

The Triose Phosphate Isomerase (TPI) Activity Colorimetric Assay Kit (BioVision, USA) was applied to monitor the activity of *Pf*TPI protein (PF3D7_1439900). Purified *Pf*TPI protein (0.5 μg) was first incubated with different concentrations of chloroquine (0-100 μM) at 28 ℃ for 1 h. The resulting mixture was then transformed into a 96-well plate, and the reaction mix buffer (including TPI substrate, developer and Enzyme Mix) was then added, followed by continuous detection of absorbance at 450 nm with a multimode plate reader (PerkinElmer, USA). The reaction buffer with chloroquine but no *Pf*TPI served as negative control. The measurements were carried out in triplicate.

Fluorescence Imaging assay

P. falciparum parasites (unsynchronized) were cultured as above mentioned in 24-well plate to ~ 5% parasitemia with 2% hematocrit and treated with DMSO or drugs for 1 h. Then fixed with 4% paraformaldehyde and 0.004% glutaraldehyde at 37 ℃ for 15min and wash with 1 × PBS for 3 times later. The parasites were resuspended with 200 μL of 1 × PBS and dripped onto coverslips precoated with 0.01% (w / w) polylysine. Following, the cells were permeabilized for 10min with 0.1% Triton-X in 37 ℃. Then, the click reaction was carried with fluorescence dye for 1 h. And the coverslips were transferred to the glass slide coated with DAPI sealing agent and imaged with Leica TCS SP8 SR confocal fluorescence microscopy. For subcellular co-localization assay, after treated with probe, parasites were incubated with organelle-specific dyes (MitoTracker™ Deep Red FM, Invitrogen; Lyso-Sensor Green, YEASEN). The subsequent operation was as described above. For co-localization of target proteins, after click reaction, parasites were incubated with the indicated primary antibody and secondary fluorescent antibody and imaged with Dragonfly 200 Spinning Disk Confocal Microscopy.

Surface plasmon resonance (SPR) assay

Multi-cycle kinetics were run on a Biacore T200 instrument to investigate the binding kinetics of CQ against the *Pf*LDH, *Pf*OAT, *Pf*PyrK, *Pf*PGK and *Pf*TPI proteins. The flow cell temperature was 25 ℃. Normalized steady-state binding curves from SPR showing binding of CQ to proteins immobilized on the CM5 Series S sensor chip (Cytiva Life Sciences) surface. Different dilutions of CQ were flowed over the

CM5 Series S sensor chip surface at 30 μL/minute for 60 seconds followed by 120 seconds of dissociation flow. Data from single cycle kinetics were analyzed using BIAevaluation software. All curves base lines were adjusted to zero, and injection start times were aligned. The reference sensorgrams was subtracted from the experimental sensorgrams to generate curves representing specific binding. A 1 : 1 binding model (Langmuir) was used to evaluate the binding kinetics to obtain the association rate constant (k_a) and dissociation rate constant (k_d). Binding affinity (K_D) was estimated based on the concentration dependence of the observed steady-state responses.

Molecular docking model

The 3D structure file of chloroquine was downloaded from PubChem. The structures of *Pf*LDH (PDB: 3ZH2), *Pf*PyrK (PDB: 6KSH), *Pf*OAT (PDB: 1LX9), *Pf*PGK (PDB: 3OZ7) and *Pf*TPI (PDB: 1M7P) were downloaded from RCSB PDB. The AutoDock tool (ADT) was used to handle these structure files and transfer their format into PDBQT. Then, the AutoDock Vina (v1.1.2) was employed for docking chloroquine to the substrate binding site of each target protein. The grid box was centered to each binding sites with the same size (size_x = 30, size_y = 30, size_z = 30). The exhaustiveness parameter was set to 10 to find a better binding pose with lower affinity score.

Results

Design and synthesis of CQ activity-based protein profiling probes

We used the strategy of photo-affinity labeling (PAL) for chloroquine probe (CQP) design [21, 22]. Our synthesis of CQP began with the conversion of 1,4-dibromopentane **1** to tert-butyl (4-aminopentyl) carbamate **2** via a nucleophilic substitution, hydrogenation and Boc-protected sequence. The treatment of **2** with 4,7-dichloroquinoline in DMSO at 130 ℃ followed by deprotection generated diamine **3**. Borch reduction of diamine **3** with acetaldehyde synthesized **4**, which was further subject to esterification and nucleophilic substitution with sodium azide to generate **5**. The click reaction of azide **5** with **6** finally produced **CQP** (Scheme 1). Notably, the CQP still retain the quinoline ring system, the chlorine at the 7-position and the terminal amino group that are indispensable for its antimalarial activity [6, 7].

Fluorescence labelling of CQP targets in parasites

Firstly, we tested the antimalarial activity of the CQP *in vitro* on *P. falciparum* 3D7 strain and confirmed that the derivatized probe CQP killed *P. falciparum* 3D7 strain in the nanomole range, retaining the antimalarial activity of chloroquine (Fig. 1b). The photo-reactive group on CQP can generate a highly active carbene chemical species, which would covalently cross-link with the target proteins upon UV irradiation (λ = 365 nm). Next, the samples can be further labeled with a TAMRA fluorescent tag through click chemistry reaction, as depicted in Fig. 1a. We went on to carry out fluorescence labeling experiments *in situ* and in the parasite lysate, respectively. As shown in Fig. 1c and d, parasite proteins were labeled with TAMRA in a CQP dose-dependent manner after UV light irradiation either *in situ* or in lysate. There

was hardly any fluorescence labeling of parasite proteins without UV-irradiation. Importantly, when pre-incubated with excess CQ, the fluorescent labeling was diminished (Fig. 1e), indicating that CQP and CQ share the same protein targets. Furthermore, the distribution of the drug in the parasite was evaluated in a live cell imaging experiment with confocal microscopy and the results showed that the drug can quickly accumulate inside the parasites, and can be competed away by excess chloroquine, which is consistent with the fluorescent labeling result (Fig. 1f). In summary, the active photo-affinity chloroquine analog probe CQP maintains the antimalarial activity and the intracellular accumulation characteristics of chloroquine. Meanwhile, it opens up the possibility to use this derivatized CQP probe to track the binding of the drug and the proteins, and to identify the target proteins.

Identification of chloroquine targets with CQP

We decided to use this CQP probe to retrieve and identify the target proteins of chloroquine. To identify these CQP-binding proteins, the parasite lysate was incubated with CQP or DMSO vehicle in the presence or absence of CQ, followed by UV-irradiation and biotin moiety incorporation through the alkynyl tag-mediated click reaction. The CQP-binding targets were then retrieved by biotin-streptavidin affinity purification and identified by quantitative proteomics. The TMT-based multiplexing scheme was chosen for parallel analysis of samples from three different treatment conditions, in order to improve statistical power (Fig. 1a). We identified a total of 40 proteins that were specifically photo-crosslinked with CQP, which was inhibited in the presence of excess CQ (Fig. 1g, S1). The detailed information of these proteins was shown in Table S1.

Identification of chloroquine targets using MS-CETSA

We also used MS-CETSA, a recently developed proteome-wide and label-free target deconvolution method based on the biophysical principle that the thermal stability of target proteins tend to shift upon binding with drugs/compounds, to identify the target proteins of CQ (Fig. 2a) [23, 24]. By monitoring the impact of CQ in various concentrations (0 ~ 300 μM) on the thermostability of the malarial proteome under different heating conditions (37 ℃, 52 ℃, 61 ℃), we identified 83 candidate interacting proteins out of a total measurement of 3375 parasite proteins (Fig. 2b). Together, we identified 8 proteins as the most potential hits which were commonly identified by both ABPP and MS-CETSA methods (Fig. 2c). Interestingly, the majority of them are involved in glycolysis and energy metabolism (Fig. 2d).

Binding and functional verification of the CQ target proteins in vitro

We then went on to verify some of these interactions in detail, focusing on five enzymes involved in glycolysis and energy metabolism – L-lactate dehydrogenase (*Pf*LDH, *PF3D7_1324900*), ornithine aminotransferase (*Pf*OAT, *PF3D7_0608800*), pyruvate kinase (*Pf*PyrK, *PF3D7_0626800*), phosphoglycerate kinase (*Pf*PGK, *PF3D7_0922500*) and triosephosphate isomerase (*Pf*TPI, *PF3D7_1439900*). To start with, we retrieved the structures of these five proteins from PDB database and modelled the binding poses of CQ to them through molecular docking simulation (Fig. 3). Interestingly, in

all cases, CQ binding was at or close to the pocket of substrate/active sites, implying the biological relevance of the binding events.

Next, the five proteins were recombinantly expressed in *E.coli* and successfully purified. As expected, CQP was photo-crosslinked to these five enzymes in a dose-dependent manner (Fig. 4a, b), which was diminished by CQ pre-treatment (Fig. 4c). Similar results were also obtained using the specific antibodies of these proteins (Fig. 4d). In addition, we measured the binding affinity between CQ and the five proteins by BIAcore surface plasmon resonance (SPR). All the measured binding events were at the level of low-μM ($K_{CQ-PfLDH}$ = 0.32 μM, $K_{CQ-PfOAT}$ = 1.91 μM, $K_{CQ-PfPyrK}$ = 0.85 μM, $K_{CQ-PfPGK}$ = 1.95 μM, $K_{CQ-PfTPI}$ = 1.18 μM, respectively) (Fig. 4e-i, S4). More importantly, the catalytic activities of these enzymes could be largely inhibited by CQ in a dose-dependent manner (Fig. 5a-e). In summary, all these experimental evidences supported the functional binding of CQ to these five parasite enzymes involved in glycolysis and energy metabolism.

CQ disrupts glycolysis and energy metabolism of parasites

Subsequently, we conducted Gene Ontology enrichment analysis on the target proteins commonly identified in ABPP and MS-CETSA strategy, and the result also suggested that CQ could disrupt the glycolytic and energy metabolic processes of parasite to exert antimalarial effects (Fig S2-S3). We also carried out immunofluorescence experiments with spinning disk confocal microscopy and confirmed that the CQP probe indeed co-localized with the relevant target proteins inside parasite (Fig. 5f). In addition, the subcellular localization analysis showed the accumulation of CQP probe in the parasites, especially in the digestive vesicles and mitochondria (Fig. 5g). Our results therefore suggested a new working mechanism that after accumulation in parasite, CQ directly targets and modulates glycolysis and energy metabolism-related proteins to exert antimalarial effects.

Discussion

In summary, we found that chloroquine could disrupt glycolysis and energy metabolism of malarial parasites through direct binding with some of the key enzymes, a new mechanism that is different from its known inhibitory effect of hemozoin formation. To the best of our knowledge, this is the first report of identifying the chloroquine antimalarial targets by a parallel usage of labeled (ABPP) and label-free (MS-CETSA) methods. Even though we mainly focused on the shared protein targets from the two methods in this work, the other candidates identified by only one of the methods might also be worthy of detailed analysis in future studies. Of note, in the development of this paper, Wirjanata *et al*. disclosed an MS-CETSA dataset with however limited proteome coverage, reporting a sole hit protein falcilysin (*PF3D7_1360800*) [25]. In our dataset, falcilysin as well as other hemoglobin proteolytic enzymes including plasmepsin Ⅱ and plasmepsin Ⅳ also showed significant thermal shift. On the other hand, multidrug resistance protein 1 (*Pf*MDR1, *PF3D7_0523000*) was identified as an interacting hit protein in our ABPP dataset, which has been demonstrated in previous study [26]. It should be noted that chloroquine is also used to treat autoimmune disorders, such as rheumatoid arthritis and lupus

erythematosus. Therefore, the reagents and approaches developed in this study can guide the future research of the MoA of chloroquine in those conditions.

Conclusion

This work discovered and proposes a new working mechanism of the antimalarial drug CQ, which is different from the past understandings. It is of great significance to alleviate the resistance of CQ in malaria treatment and expand the use of CQ for new indications. The knowledge gained from this systematic protein target profiling study provided new direction for the development of new quinoline scaffold-based drugs. In addition, this work established a new research strategy for the MoA study of other important but not-well-understood drugs.

Abbreviations

CQ
chloroquine
MoA
mechanism of action
ABPP
activity-based protein profiling
MS-CETSA
mass spectrometry-coupled cellular thermal shift assay
DV
digestive vacuole
LDH
lactate dehydrogenase
PAL
photo-affinity labelling
CQP
chloroquine probe
DMSO
dimethyl sulfoxide
OAT
ornithine aminotransferase
PyrK
pyruvate kinase
PGK
phosphoglycerate kinase
TPI
triosephosphate isomerase

IC50
half-maximal inhibitory concentration
AUC
area under the curve
MAD
median absolute deviation
FC
fold change
MDT
mininal dose threshold
SPR
Surface plasmon resonance

Declarations

Acknowledgements

This work was funded by the National Natural Science Foundation of China (82074098 and 81841001); the National Key R&D Program of China (2020YFA0908000, 2020YFA0908004 and 2020YFA0908001) and the Fundamental Research Funds for the Central public welfare research institutes (ZZ13-ZD-07, ZZ14-YQ-050, ZZ14-YQ-051, ZZ14-ND-010, ZZ15-ND-10).

Author Contributions

J.W., L.D., and C.X. conceived and designed the experiments. P.G. and Y.L. performed the major experiments. F.X. performed the synthesis of probe. J.C., L.G., F.Y., L.Z., J.Z., Q.Z., Z.L., Y.M., Y.Z., executed other experiments and bioinformatic analyses. L.D., C.X., P.G., Y.L. and W.X. wrote the manuscript. All authors have reviewed and edited the manuscript. and agreed with the content of the manuscript.

Conflict of interest

The authors declare that they have no conflict of interest.

References

1. Morello JA. Clinical Microbiology Reviews: genesis of a journal. Clin Microbiol Rev. 1999;12(2):183-6.

2. Phillips MA, Burrows JN, Manyando C, van Huijsduijnen RH, Van Voorhis WC, Wells TNC. Malaria. Nat Rev Dis Primers. 2017;3:17050.

3. World Health Organization, World Malaria Report 2020; https://www.who.int/publications/i/item/9789240015791, 2020.

4. Ashley EA, Phyo AP. Drugs in Development for Malaria. Drugs. 2018;78(9):861-79.

5. Zhou W, Wang H, Yang Y, Chen ZS, Zou C, Zhang J. Chloroquine against malaria, cancers and viral diseases. Drug Discov Today. 2020.

6. Thomé R, Lopes S, Costa F, Verinaud L. Chloroquine: modes of action of an undervalued drug. Immunology letters. 2013;153:50-7.

7. Ecker A, Lehane A, Fidock DA. Treatment And Prevention Of Malaria: Antimalarial Drug Chemistry, Action And Use. Springer. 2012.

8. Homewood CA, Warhurst DC, Peters W, Baggaley VC. Lysosomes, pH and the anti-malarial action of chloroquine. Nature. 1972;235(5332):50-2.

9. Djimde A, Doumbo OK, Cortese JF, Kayentao K, Doumbo S, Diourte Y, et al. A molecular marker for chloroquine-resistant falciparum malaria. N Engl J Med. 2001;344(4):257-63.

10. Miller LH, Ackerman HC, Su XZ, Wellems TE. Malaria biology and disease pathogenesis: insights for new treatments. Nat Med. 2013;19(2):156-67.

11. Kaur K, Jain M, Reddy R, Jain R. Quinolines and structurally related heterocycles as antimalarials. European journal of medicinal chemistry. 2010;45(8):3245-64.

12. Read JA, Wilkinson KW, Tranter R, Sessions RB, Brady RL. Chloroquine Binds in the Cofactor Binding Site ofPlasmodium falciparum Lactate Dehydrogenase. Journal of Biological Chemistry. 1999;274(15):10213-8.

13. Wang J, Zhang CJ, Chia WN, Loh CC, Li Z, Lee YM, et al. Haem-activated promiscuous targeting of artemisinin in Plasmodium falciparum. Nat Commun. 2015;6:10111.

14. Wang J, Zhang J, Shi Y, Xu C, Zhang C, Wong YK, et al. Mechanistic Investigation of the Specific Anticancer Property of Artemisinin and Its Combination with Aminolevulinic Acid for Enhanced Anticolorectal Cancer Activity. ACS Cent Sci. 2017;3(7):743-50.

15. Chen X, Wang Y, Ma N, Tian J, Shao Y, Zhu B, et al. Target identification of natural medicine with chemical proteomics approach: probe synthesis, target fishing and protein identification. Signal Transduct Target Ther. 2020;5(1):72.

16. Capci A, Lorion MM, Wang H, Simon N, Leidenberger M, Borges Silva MC, et al. Artemisinin-(Iso)quinoline Hybrids by C-H Activation and Click Chemistry: Combating Multidrug-Resistant Malaria. Angew Chem Int Ed Engl. 2019;58(37):13066-79.

17. Martinez Molina D, Jafari R, Ignatushchenko M, Seki T, Larsson EA, Dan C, et al. Monitoring drug target engagement in cells and tissues using the cellular thermal shift assay. Science.

2013;341(6141):84-7.

18. Dai L, Zhao T, Bisteau X, Sun W, Prabhu N, Lim YT, et al. Modulation of Protein-Interaction States through the Cell Cycle. Cell. 2018;173(6):1481-94 e13.

19. Dai L, Prabhu N, Yu LY, Bacanu S, Ramos AD, Nordlund P. Horizontal Cell Biology: Monitoring Global Changes of Protein Interaction States with the Proteome-Wide Cellular Thermal Shift Assay (CETSA). Annu Rev Biochem. 2019;88:383-408.

20. Lu KY, Quan B, Sylvester K, Srivastava T, Fitzgerald MC, Derbyshire ER. Plasmodium chaperonin TRiC/CCT identified as a target of the antihistamine clemastine using parallel chemoproteomic strategy. Proc Natl Acad Sci U S A. 2020;117(11):5810-7.

21. Mackinnon AL, Taunton J. Target Identification by Diazirine Photo-Cross-linking and Click Chemistry. Curr Protoc Chem Biol. 2009;1:55-73.

22. Li Z, Hao P, Li L, Tan CY, Cheng X, Chen GY, et al. Design and synthesis of minimalist terminal alkyne-containing diazirine photo-crosslinkers and their incorporation into kinase inhibitors for cell- and tissue-based proteome profiling. Angew Chem Int Ed Engl. 2013;52(33):8551-6.

23. Dziekan JM, Wirjanata G, Dai L, Go KD, Yu H, Lim YT, et al. Cellular thermal shift assay for the identification of drug-target interactions in the Plasmodium falciparum proteome. Nat Protoc. 2020;15(6):1881-921.

24. Dziekan JM, Yu H, Chen D, Dai L, Wirjanata G, Larsson A, et al. Identifying purine nucleoside phosphorylase as the target of quinine using cellular thermal shift assay. Science translational medicine. 2019;11(473).

25. Wirjanata, G.; Dziekan, J.; Lin, J.; Sahili, A. E.; Bozdech, Z., Identification of an inhibitory pocket in falcilysin bound by chloroquine provides a new avenue for malaria drug development. Preprint at bioRxiv doi: 10.1101/2021.04.08.438947, (2021).

26. Vezmar M, Georges E. Direct binding of chloroquine to the multidrug resistance protein (MRP): possible role for MRP in chloroquine drug transport and resistance in tumor cells. Biochemical pharmacology. 1998;56(6):733-42.

Figures

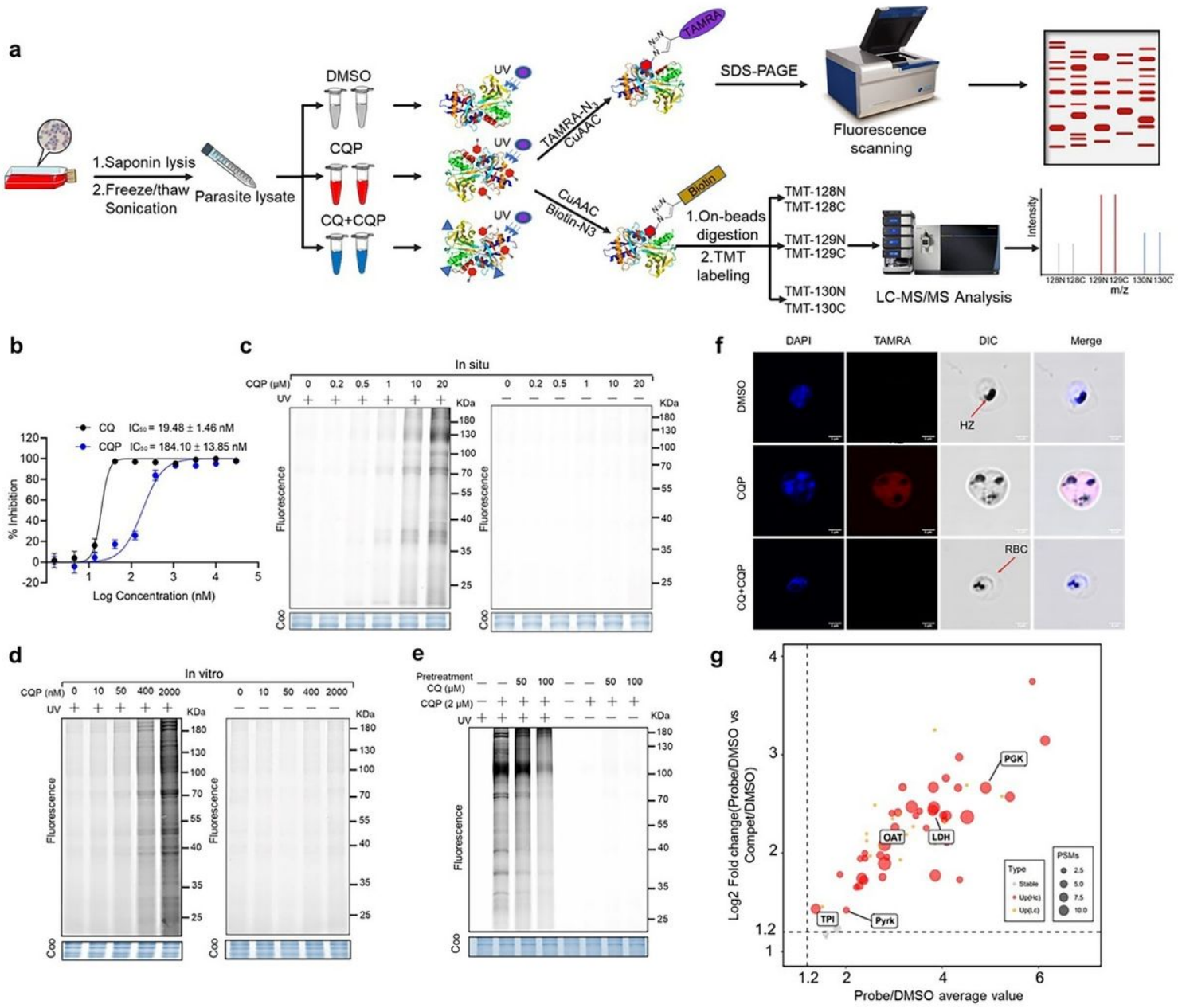

Figure 1

The identification of chloroquine target proteins by CQP through ABPP. (a) General workflow of ABPP used to identify chloroquine target proteins with photoaffinity probe. Parasite lysates were incubated with probe, drug or vehicle followed by irradiation with UV light (λ = 365 nm). The alkyne tag allows for the subsequent attachment of a fluorescent tag or biotin moiety through click chemical reaction. The fluorescence labeling of parasite proteins is visualized by fluorescence scanning after resolving on SDS-PAGE gel. The pull-down of CQP-interacting proteins by biotin-streptavidin affinity purification is subject to TMT-based labeling and quantification on LC-MS/MS. (b) The determination of antimalaria activity of CQP and CQ in P. falciparum 3D7 strain. (c, d) The in situ and in vitro labeling of many parasite proteins exhibits in were labeled in a dose-dependent manner after UV irradiation, while there was no labeling without UV irradiation. (e) The labeling of CQP-target proteins in parasite lysate can be competed with

excess CQ. (f) Confocal microscopy showing the distribution of CQP inside the P. falciparum 3D7 parasites (HZ = hemozoin, RBC = red blood cell). (g) Scatter plot of 60 quantified proteins from CQP ABPP experiment. Each dot represents a quantified protein, with the x-axis represents the mean of log2 protein abundance difference between CQP and DMSO control group, while y-axis represents the mean of log2 difference between CQP and CQ+CQP group. Two biological replicates were included in the experiment. The dashed line represents the fold change cutoff criteria (> 1.2) used for hit selection. The gray points represent proteins with Padj >0.05. The proteins measured with only 1 PSM were regarded as low-confidence, and colored in orange color. The remaining 40 proteins were kept as high-confidence targets and colored in red and the dot size is proportional to the associated PSM numbers.

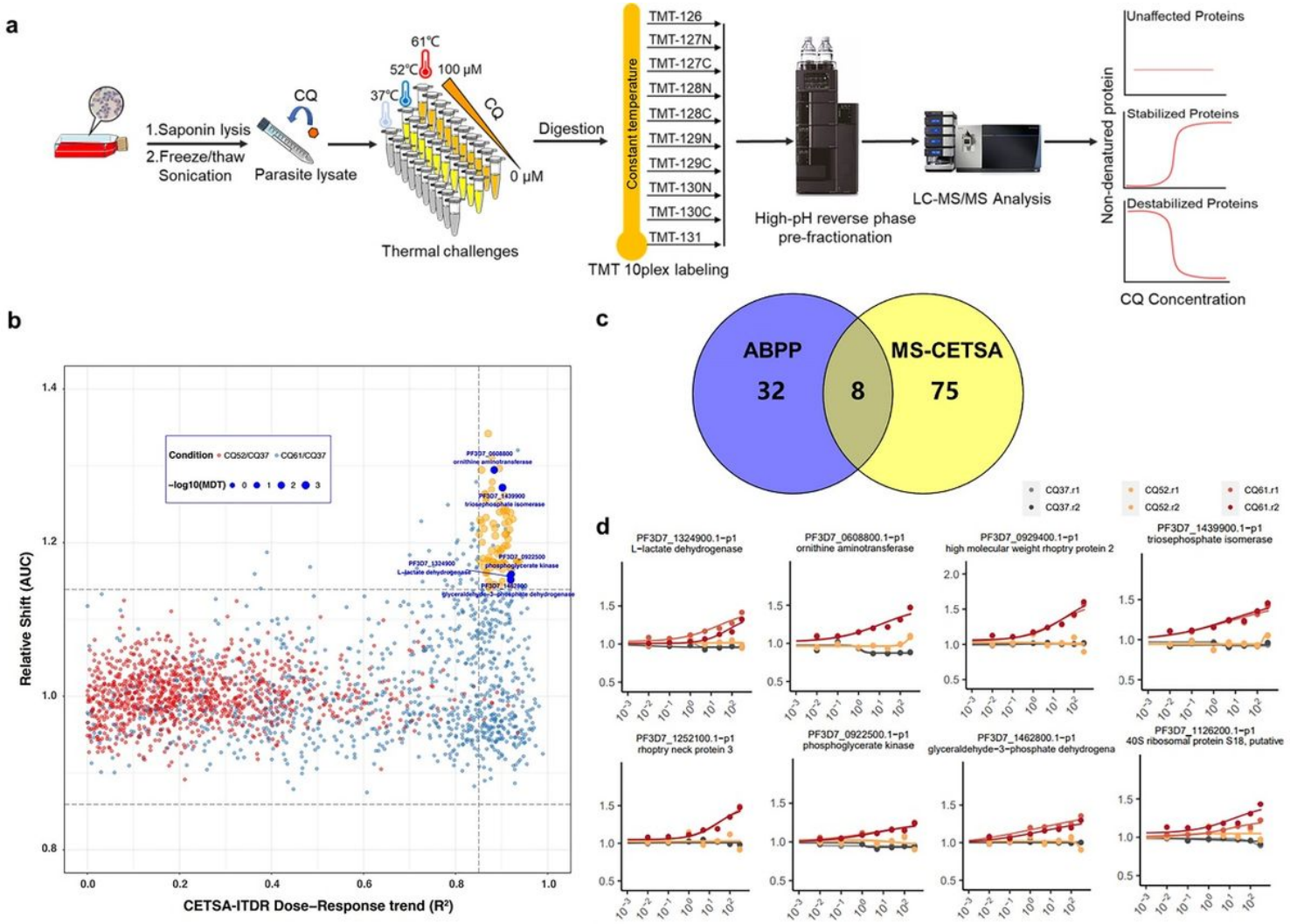

Figure 2

The identification of chloroquine target proteins through MS-CETSA. (a) General workflow of MS-CETSA used to identify chloroquine interacting protein. Parasite lysates were incubated with CQ at various concentrations, followed by heating under different temperature conditions. The remaining soluble proteins were collected for LysC/Trypsin digestion. The digested peptides are labeled by TMT10plex reagent and quantified by mass spectrometry. The profile of protein thermal stability along the CQ concentration gradient were generated. The proteins with significant thermal shifts were identified as the

potential CQ-targeting proteins. (b) A R2-AUC plot showing the protein thermal stability shift of the whole P. falciparum proteome after incubation with 0-300 □M chloroquine from the lysate MS-CETSA-ITDR experiment. (c) Venn diagram showing the overlap of target proteins identified in ABPP and MS-CETSA. (d) Thermal shift profile of the 8 overlap target proteins.

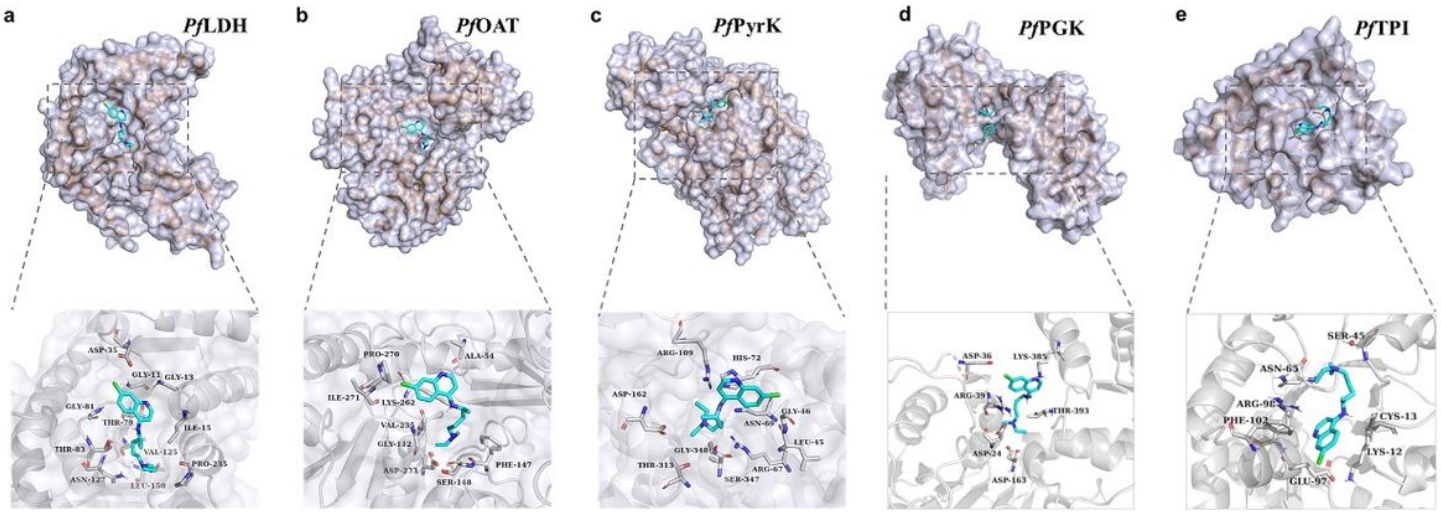

Figure 3

Docking simulation of CQ binding to PfLDH (a), PfOAT (b), PfPyrK (c), PfPGK (d) and PfTPI (e) proteins, respectively. The calculated binding affinities (kcal/mol) are -6.2, -6.1, -6.5, -5.8 and -5.7 for PfLDH, PfOAT, PfPyrK, PfTPI and PfPGK, respectively.

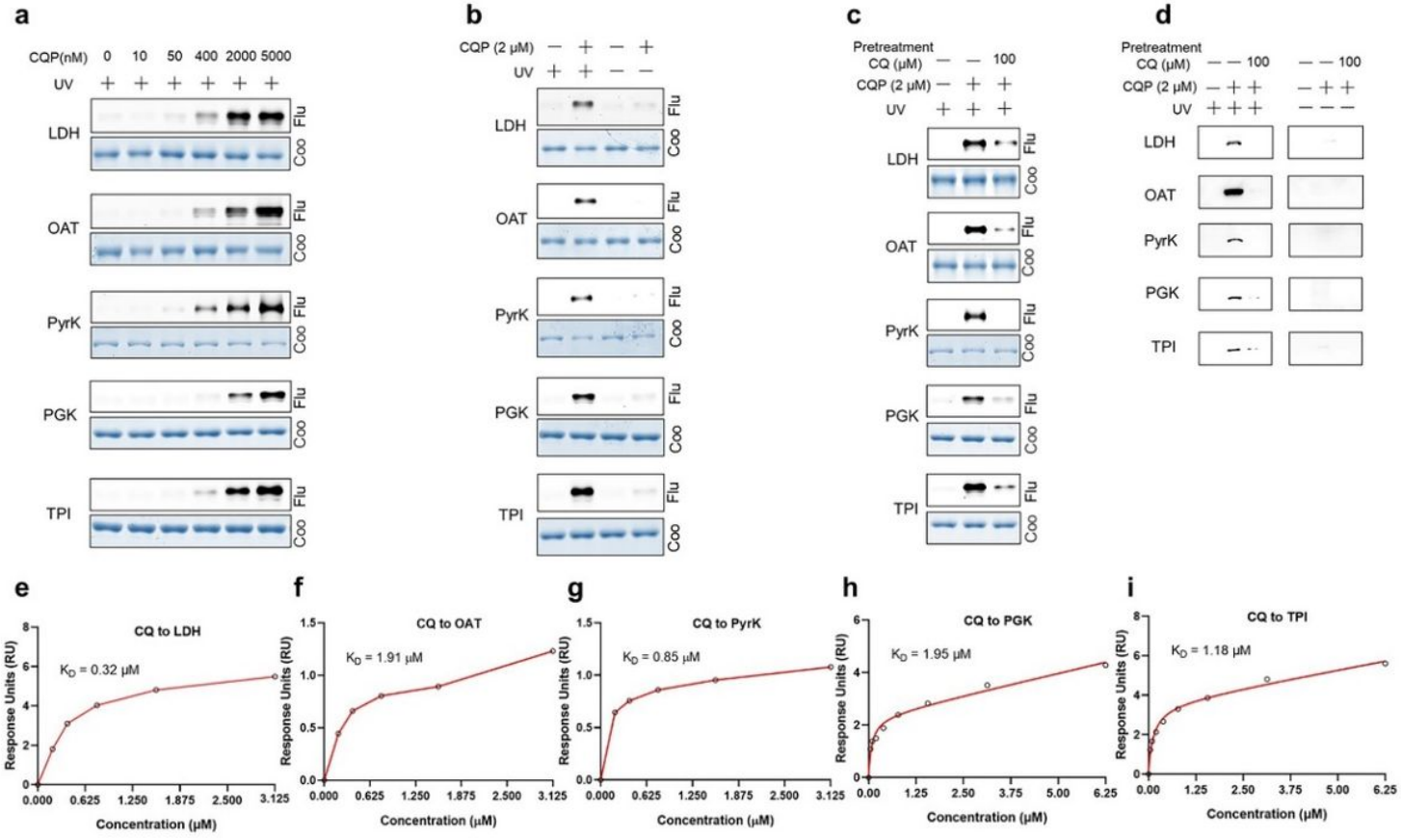

Figure 4

Binding verification of the CQ target protein in vitro. (a) CQP specifically binds to recombinant PfLDH, PfOAT, PfPyrK, PfPGK, and PfTPI proteins in a dose-dependent manner. (b) There was no binding between CQP and recombinant parasite proteins without UV irradiation. (c) Excess CQ (50 ×) pre-treatment can compete with the CQP binding to the target proteins. (d) Validation of the specific targeting of CQP to the 5 target proteins in parasites by western blot. (e, f, g, h, i) The determination of binding affinity of chloroquine with the 5 target proteins through SPR assay.

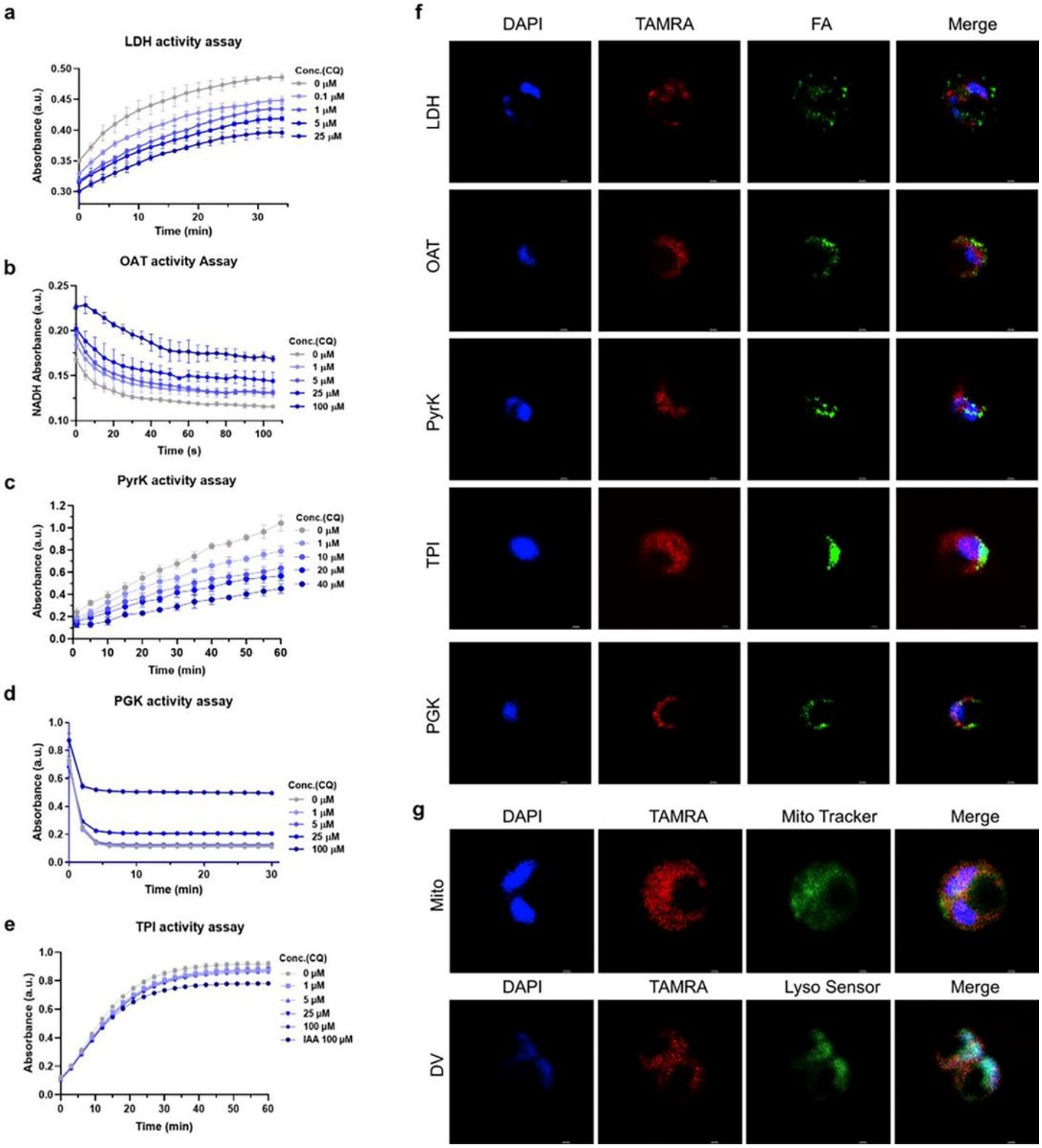

Figure 5

Functional verification of the CQ target protein in vitro. (a, b, c, d, e) Chloroquine inhibits the enzymatic activities of the PfLDH (a), PfOAT (b), PfPyrK (c), PfPGK (d) and PfTPI (e) in vitro in a dose-dependent manner. (f) Immunofluorescence colocalization experiment of target protein and probe (FA : Fluorescent Antibody). (g) Subcellular localization of CQP (DV : digestive vacuole, Mito : mitochondria).

Supplementary Files

This is a list of supplementary files associated with this preprint. Click to download.

- Scheme1.png
- Supplementaryfile211116.pdf